J. Pharm. Pharmacol. 1992, 44: 396–401
Received September 6, 1991

Demonstration of the Receptor-mediated Hepatic Uptake of Dextran in Mice

MAKIYA NISHIKAWA, FUMIYOSHI YAMASHITA, YOSHINOBU TAKAKURA, MITSURU HASHIDA AND HITOSHI SEZAKI

Department of Basic Pharmaceutics, Faculty of Pharmaceutical Sciences, Kyoto University, Sakyo-ku, Kyoto 606, Japan

Abstract—To establish a rationale of designing a drug targeting system using dextran conjugation, the disposition behaviour of dextran itself was investigated in mice. At a high dose (100 mg kg^{-1}), [^{14}C]dextran was retained in the blood circulation for a considerably long period. However, [^{14}C]dextran rapidly disappeared from the plasma and accumulated in the liver (up to 60% of dose in 1 h) after a dose of 1 mg kg^{-1}. Cellular localization of [^{14}C]dextran in the liver following intravenous administration was examined and the contribution of parenchymal cells was demonstrated as well as the case of galactosylated bovine serum albumin (Gal-BSA). Pharmacokinetic analysis based on a physiological model including Michaelis–Menten type uptake mechanisms revealed that the Michaelis constant $K_{m,l}$ of [^{14}C]dextran was 100 times greater than that of Gal-BSA. Coadministration of Gal-BSA delayed the hepatic uptake of [^{14}C]dextran and the simulation based on the physiological model suggested that [^{14}C]dextran was taken up by the same mechanism as Gal-BSA. These results suggested that dextran conjugation of a drug might lead to its undesirable accumulation in the liver at a low dose and an appropriate modification of dextran, such as carboxymethylation, would be required in such cases.

The chemical conjugation of highly active anticancer and peptide drugs with macromolecular carriers seems to offer a promising way to optimize their delivery, since macromolecules are highly diverse in their physicochemical properties and biological functions (Sezaki & Hashida 1984; Vogel 1988; Sezaki et al 1989). In these approaches, the disposition behaviour of the conjugated drug is altered depending on the properties of the carrier macromolecules; it is therefore appropriate to investigate the in-vivo fate of such macromolecules.

Dextran has many advantages for this strategy, including high water solubility, multiple hydroxyl groups readily modified chemically, low immunogenicity, and long experience in clinical use as a plasma expander. From these viewpoints, dextran itself is considered to be a biologically inert modifier with a high molecular weight (mol. wt). In our series of investigations, we have developed various kinds of conjugates of anticancer agents (Hashida et al 1984; Takakura et al 1987a, b) and biologically active proteins (Takakura et al 1989a, b; Fujita et al 1990b) with neutral, cationic, and anionic dextran derivatives. We have revealed that the molecular size and electric charge of dextran derivatives are major determinants in the distribution of the conjugates (Takakura et al 1990). For example, anionic carboxymethyldextran and its drug conjugates slowly disappeared from the blood circulation after intravenous injection. Neutral dextran also showed long retention in the blood at a high dose (100 mg kg^{-1}). On the other hand, cationic diethylaminoethyldextran and its conjugates were rapidly taken up by the tissue, in particular, by the liver. These results were explained by electrostatic interaction between the macromolecule and the biological organism. However, the modification of uricase with dextran resulted in an increase of liver uptake at a low dose (Fujita et al 1990b). Mowry & Millican (1953) studied distribution of dextran histochemically in mice and showed that dextran was taken up by several organs such as the liver, kidney, spleen, and lung.

In the present study, therefore, the disposition properties of dextran, especially the uptake process by the liver, were studied in mice.

Correspondence: H. Sezaki, Department of Basic Pharmaceutics, Faculty of Pharmaceutical Sciences, Kyoto University, Sakyo-ku, Kyoto 606, Japan.

Materials and Methods

Chemicals

Dextran with average mol. wt of approximately 70 kDa (T-70) was purchased from Pharmacia, Uppsala, Sweden. Bovine serum albumin (BSA; fraction V) was obtained from Nacalai Tesque, Tokyo, Japan. Potassium [^{14}C]cyanide was supplied by Amersham Japan, Tokyo. Collagenase (type I) was obtained from Sigma, St Louis, MO. All other chemicals were reagent grade products obtained commercially.

Animals

Male ddY mice, 25–28 g, were obtained from the Shizuoka Agricultural Co-operative Association for Laboratory Animals, Shizuoka, Japan.

Radiolabelling of dextran

[Carboxyl-^{14}C]dextran (T-70) was prepared according to the method of Isbell et al (1957) with slight modification. Briefly, 0·05 mmol of dextran (T-70), sodium bicarbonate, and sodium hydroxide was dissolved in 5 mL of distilled water and frozen in a glass tube. Potassium [^{14}C]cyanide (0·05 mmol) was added and the tube was heat-sealed. The mixture was thawed and stored at 45°C for 24 h, then heated for 7 h at 50°C in a stream of air to effect hydrolysis. The product was purified by gel filtration using a Sephadex G-25 (Pharmacia, Uppsala, Sweden) column and concentrated by ultrafiltration. The specific activity of dextran (T-70) was 0·025 MBq mg^{-1}.

Synthesis of galactosylated BSA

Galactosylated BSA (Gal-BSA) was synthesized according to the method of Lee et al (1976). In brief, 2-imino-2-methoxyethyl 1-thiogalactoside (IME-thiogalactoside) was obtained from cyanomethyl 2,3,4,6-tetra-*O*-acetyl-1-thiogalactosides (CNM-thiogalactosides) by de-*O*-acetylation and mixed with BSA in 50 mM borate buffer (pH 9·5) for 8 h at room temperature (21°C). The obtained Gal-BSA was washed, concentrated by ultrafiltration against distilled water and lyophilized. About 21 galactose residues were attached to one molecule of BSA determined using trinitrobenzene sulphonic acid (TNBS).

In-vivo distribution experiment

Sample solutions were prepared by dissolving appropriate amounts of radiolabelled and unlabelled dextran in 0·9% NaCl (saline). These were then injected into the tail vein of mice at a volume of 10 mL kg^{-1} body wt. The doses of dextran were 1, 10, and 100 mg kg^{-1}. Mice were housed in metabolic cages for urine collection. At appropriate intervals after injection, blood was collected from the vena cava under ether anaesthesia and the mice were killed. The heart, lung, liver, spleen, kidney, intestine, muscle, and iliac lymph nodes (three or four nodes) were excised, rinsed with saline, weighed, and subjected to assay. Experiments were continued until the plasma concentration decreased to less than 0·1% of dose mL^{-1}; that is, until 2, 5, and 8 h after injection for experiments at 1, 10, and 100 mg kg^{-1}, respectively. Cellular localization of dextran in the liver was determined in different mice by fractioning parenchymal and nonparenchymal cells after collagenase perfusion.

Simultaneous administration of dextran and Gal-BSA

Radiolabelled dextran (1 mg kg^{-1}) was injected into mice simultaneously with 30 mg kg^{-1} of Gal-BSA. At 0·17, 0·5, 1, and 2 h after injection, blood and liver were sampled and subjected to assay.

Analytical methods

The radioactivity in plasma, urine and tissues was measured using a liquid scintillation counter (LSA-5000, Beckman, Tokyo, Japan) after dissolution in Soluene-350 (Packard, Netherlands) followed by scintillation medium, Clear-sol I (Nacalai Tesque, Tokyo, Japan).

Calculation of tissue uptake rate index and organ clearance

Tissue distribution was evaluated using a tissue uptake rate index calculated in terms of clearance as reported previously (Takakura et al 1987b). The change in the amount of radioactivity in a tissue with time can be described as follows:

$$dT(t)/dt = CL_{in}C(t) - K_{out}T(t) \quad (1)$$

where T(t) (% of dose g^{-1}) is the amount of radioactivity in 1 g of the tissue, C(t) (% of dose mL^{-1}) is the plasma concentration of radioactivity, CL_{in} ($mL\,h^{-1}\,g^{-1}$) is the tissue uptake rate index from the plasma to the tissue, and K_{out} (h^{-1}) is the efflux rate constant from the tissue. In the present study, the efflux process can be considered to be negligible since dextran was stably labelled with ^{14}C and no elimination was observed in the tissue during the experimental period. Ignoring efflux, equation 1 integrates to

$$CL_{in} = T(t1)/\int_0^{t1} C(t)dt = T(t1)/AUC_{0\text{-}t1} \quad (2)$$

According to equation 2, the tissue uptake rate index is calculated using the amount of radioactivity in the tissue at any time and the area under the plasma concentration-time curve (AUC) up to that time. Then the organ clearance (CL_{org}) is expressed as follows:

$$CL_{org} = CL_{in}W \quad (3)$$

where W (g) is the total weight of the organ. If tissue uptake process followed non-linear kinetics and CL_{in} was not constant, the calculated CL_{in} values would represent the average value for the overall experimental period. We have also calculated total body clearance (CL_{total}) from AUC for infinite time (AUC_∞) using the following equation

$$CL_{total} = Dose/AUC_\infty \quad (4)$$

This also represents the average value, if the total disposition did not follow linear kinetics.

Pharmacokinetic analysis based on a physiological model

The plasma and liver concentrations of [^{14}C]dextran (T-70) were analysed based on a model shown in Fig. 1, which is similar to that employed for the analysis of glycosylated protein (Nishikawa et al unpublished data). In this model, the body is represented by three compartments, plasma pool (BP), sinusoidal and Disse spaces in the liver (EC), and intracellular space in the liver (IC). The BP and EC compartments have apparent volumes of distribution, V_p and V_l, respectively. The BP compartment represents all spaces for plasma within blood vessels of the tissue except the liver. This compartment is connected with EC by the hepatic plasma flow (Q). The uptake of the [^{14}C]dextran (T-70) from EC to IC is expressed as a Michaelis–Menten type of saturable process with maximum uptake rate, $V_{max,l}$, and Michaelis constant, $K_{m,l}$. The extra-hepatic elimination from BP is also assumed to be a saturable process represented by $V_{max,p}$ and $K_{m,p}$. At time zero, the injected substance is assumed to be distributed in BP and EC compartments at the same concentration. Mass balance equations for the concentration of [^{14}C]dextran in BP, EC, and IC, respectively, are written as:

$$dC_p/dt = (QC_l - QC_p - V_{max,p}C_p/(K_{m,p} + C_p))/V_p \quad (5)$$

$$dC_l/dt = (QC_p - QC_l - V_{max,l}C_l/(K_{m,l} + C_l))/V_l \quad (6)$$

$$dX_l/dt = V_{max,l}C_l/(K_{m,l} + C_l) \quad (7)$$

The values of V_p, VC_l, and Q were assumed to be 1·5, 0·15 mL and 85 mL h^{-1}, respectively (Gerlowski & Jain 1983). To obtain the kinetic parameters, these equations were fitted to the experimental data by use of the non-linear least squares method MULTI associated with the Runge–Kutta–Gill method [MULTI(RUNGE)] on the mainframe computer, M-382, of the Kyoto University Data Processing Center.

Based on the assumption of the competitive inhibition in liver uptake between dextran and Gal-BSA administered simultaneously, equations 5–7 are rewritten as:

$$dC_p/dt = (QC_l - QC_p - V_{max,p}C_p/(K_{m,p} + C_p))/V_p \quad (8)$$

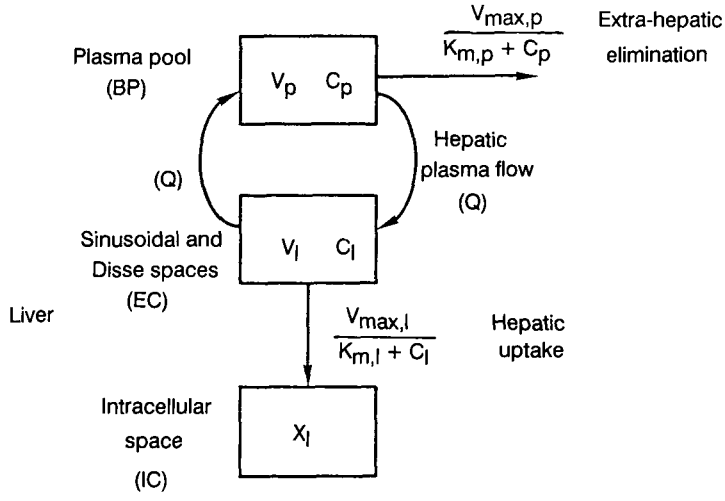

FIG. 1. Physiological pharmacokinetic model for the disposition of [^{14}C]dextran (T-70).

$$dC_I/dt = (QC_p - QC_I - V_{max,I}C_I/(K_{m,I}(1 + C_I'/K_{m,I}') + C_I))/V_I \quad (9)$$

$$dX_I/dt = V_{max,I}C_I/(K_{m,I}(1 + C_I'/K_{m,I}') + C_I) \quad (10)$$

where $K_{m,I}'$ is the Michaelis–Menten constant of Gal-BSA on liver uptake and C_I' is the concentration in EC of Gal-BSA. Employing the parameters for Gal-BSA, the plasma and liver concentrations of [^{14}C]dextran in the simultaneous administration experiment were also simulated using the Runge-Kutta-Gill method.

Results

Tissue distribution and urinary excretion of dextran

After intravenous injection of [^{14}C]dextran (T-70) to mice at a dose of 1 mg kg^{-1}, a rapid elimination of radioactivity in the plasma was observed and up to 60% of the dose was recovered in the liver after 1 h (Fig. 2). The elimination of radioactivity from the plasma and the accumulation in the liver, however, were delayed with an increase of the dose. The radioactivity in the liver did not decrease during the observation time at each dose. Urinary recovery of radioactivity at the end of the experiments was 30·5, 35·0, and 43·6% of dose for 1, 10, and 100 mg kg^{-1}, respectively, and the total recoveries in the liver and urine were over 90% at each dose. Only a little radioactivity was counted in other tissues except the kidney in the early period after the injection (data not shown).

In Fig. 2, the results of the disposition experiment of [^{111}In]Gal-BSA at doses of 1 and 10 mg kg^{-1} (Nishikawa et al unpublished data) are presented for comparison. [^{111}In]Gal-BSA was also dose dependently taken up by the liver but the rates of uptake were faster than those of [^{14}C]dextran at the same dose.

Cellular localization of [^{14}C]dextran (T-70) in the liver

The fractionation of liver cells was performed after intravenous injection of [^{14}C]dextran (T-70) at a dose of 1 mg kg^{-1}. One hour after administration, 4·82 and 1·19% of dose of [^{14}C]dextran per 10^7 cells were counted in parenchymal and nonparenchymal cells, respectively. This preferential uptake

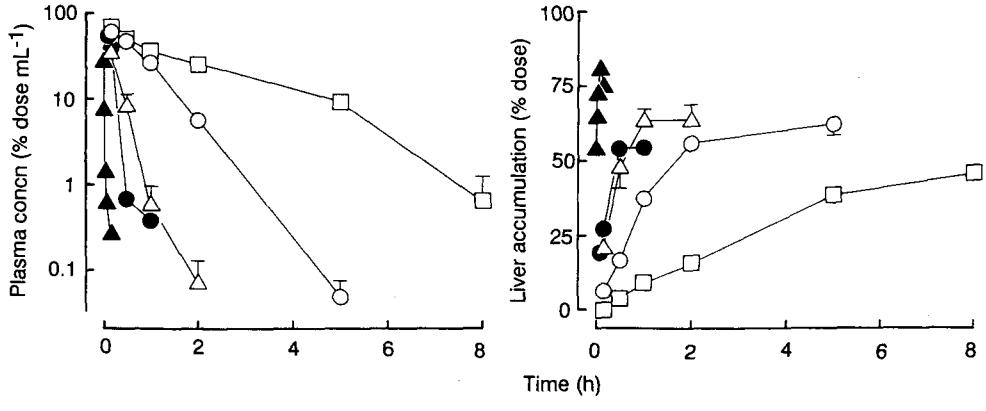

FIG. 2. Plasma concentration (A) and liver accumulation (B) of [^{14}C]dextran (T-70) after intravenous injection in mice at doses of 1 (△), 10 (○), and 100 mg kg^{-1} (□). Results are expressed as the mean ± s.d. of four mice. Results of [^{111}In]Gal-BSA at doses of 1 (▲) and 10 mg kg^{-1} (●) (Nishikawa et al unpublished data) are presented for comparison.

Table 1. Calculated AUC, clearance, and tissue uptake rate index for [^{14}C]dextran (T-70) in mice.

Dose (mg kg^{-1})	AUC (% of dose h mL^{-1})	Clearance (μL h^{-1})			Tissue uptake rate index (μL h^{-1} g^{-1})			
		CL_{total}	CL_{liver}	CL_{urine}	Liver	Spleen	Kidney	Muscle
1	17·2	5810	3730	1740	2650	35·2	30·7	8·55
10	69·4	1440	906	412	749	16·9	14·9	6·59
100	149	673	323	293	257	15·2	8·23	5·18

Table 2. Pharmacokinetic parameters of [^{14}C]dextran (T-70) and [^{111}In]Gal-BSA in mice based on a physiological model.

Compound	Liver		Blood pool	
	$K_{m,l}$ (μg mL^{-1})	$V_{max,l}$ (μg h^{-1})	$K_{m,p}$ (μg mL^{-1})	$V_{max,p}$ (μg h^{-1})
Dextran	33	150	250	400
Gal-BSA	0·31	490	11	400

Constants: $Q = 85$ mL h^{-1}, $V_p = 1{\cdot}5$ mL, $V_l = 0{\cdot}15$ mL. Parameters of Gal-BSA were obtained previously, based on the same model (Nishikawa et al unpublished data).

was similar to that found with Gal-BSA at the same dose (Nishikawa et al unpublished data) which was known to be taken up by the parenchymal cells via a receptor-mediated mechanism. The uptake ratio (PC/NPC) of 4·01 was greater than that of [^{111}In]cationized BSA (2·04) in mice which binds nonspecifically to both cell types according to their surface area ratio (Nakane et al 1988).

Calculation of basic pharmacokinetic parameters and tissue uptake rate index

Table 1 summarizes the AUC_∞, total-body, hepatic, and urinary clearances, and tissue uptake rate indices for intravenously administered [^{14}C]dextran (T-70) at three doses. The apparent hepatic clearance was very large at 1 mg kg^{-1} but decreased as the administered dose increased; total-body clearance also decreased. Tissue uptake rates in the spleen, kidney, and muscle were small compared with that of the liver and relatively constant regardless of the dose.

Pharmacokinetic analysis based on a physiological model

Equations 5–7 were simultaneously fitted to the experimental data of plasma concentration and liver accumulation at three doses and the values of $K_{m,l}$, $V_{max,l}$, $K_{m,p}$, and $V_{max,p}$ were calculated (Table 2). The simulated plasma concentration and liver accumulation curves after the injection of dextran at doses 1, 10, and 100 mg kg^{-1} were in good agreement with the experimental data at each dose (Fig. 3), suggesting that the hepatic uptake process and whole body distribution of [^{14}C]dextran (T-70) can be analysed by this physiological model. Compared with the value of $K_{m,l}$ of [^{111}In]Gal-BSA estimated from the same model (Table 2), the affinity of [^{14}C]dextran (T-70) was 100 times lower.

Competitive inhibition of hepatic uptake between [^{14}C]dextran (T-70) and Gal-BSA

When Gal-BSA (30 mg kg^{-1}) was administered with [^{14}C]dextran (T-70), the liver accumulation of dextran was markedly reduced to 0·0 and 1·0% of dose at 0·17 and 0·5 h after injection, respectively. At these times dextran had started to accumulate in the liver and at 2 h, 31·9% of dose was recovered in the liver. The plasma concentration also decreased more slowly compared with single administration, reflecting the slow accumulation in the liver. To analyse this phenomenon, the plasma concentration and liver accumulation curves of [^{14}C]dextran after simultaneous administration were simulated using the present model with the values listed in Table 2. Simulation was performed assuming that dextran and Gal-BSA competitively inhibited each other only in the liver uptake process. Fig. 4 compares computer simulation curves and in-vivo distribution data. The two curves were in good agreement with experimental data.

Discussion

It is important to elucidate the disposition characteristics of carrier macromolecules in the strategy of optimizing drug disposition using chemical modification with macromole-

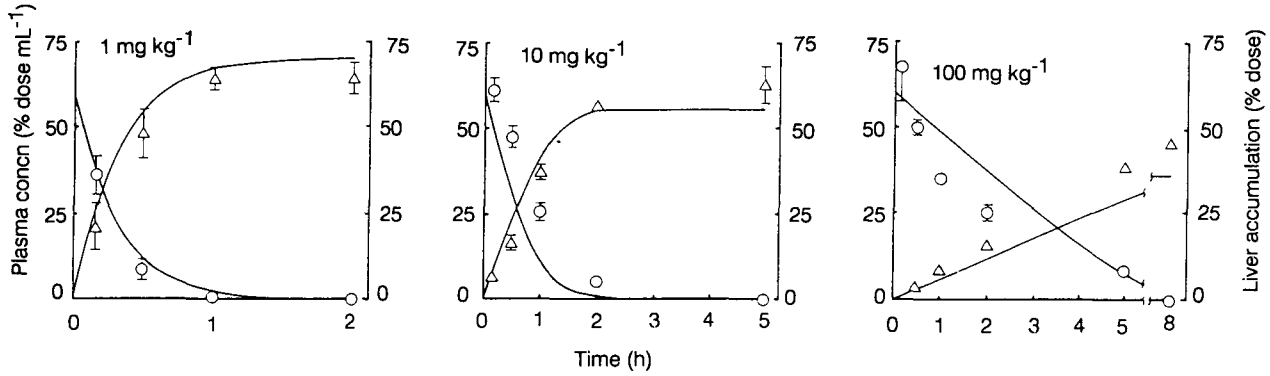

FIG. 3. Multiple curve-fitting of plasma concentration (○)- and liver accumulation (△)-time profiles of [^{14}C]dextran (T-70). The simulated curves were calculated based on equations 5–7 using the parameters listed in Table 2.

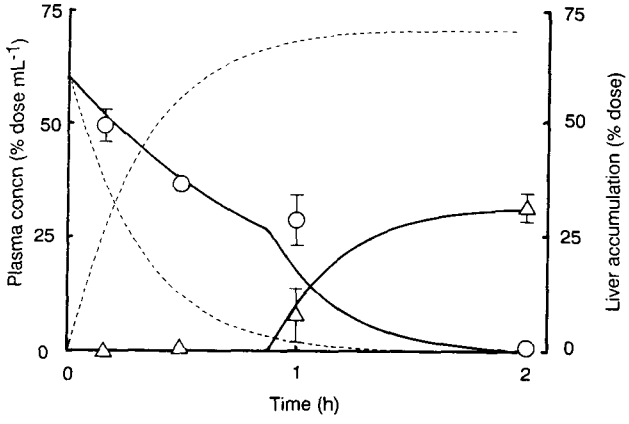

FIG. 4. Effect of coadministration of Gal-BSA (30 mg kg^{-1}) on plasma concentration (○) and liver accumulation (△) of [^{14}C]dextran (1 mg kg^{-1}). The solid curves were calculated based on the equations 8–10 using the parameters listed in Table 2. The dashed curves represent the simulations after a single administration of dextran.

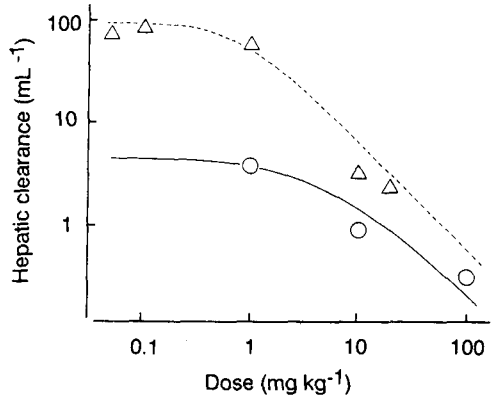

FIG. 5. The relationship between apparent hepatic clearance and administered dose of [^{14}C]dextran in mice. The curve represents the hepatic clearance based on equations 5–7 using the parameters listed in Table 2. Each point (○) represents experimental data calculated by dividing total amount of [^{14}C]dextran accumulated in the liver by plasma AUC. Results of [^{111}In]Gal-BSA are shown for comparison (△, dashed curve).

cules. In our previous study, it was revealed that the size and charge of dextran derivatives controlled their disposition behaviour at the high dose of 100 mg kg^{-1} (Takakura et al 1990); receptor-mediated uptake was not recognized. However, the biological recognition of dextran and its derivatives could be detected only at doses sufficiently lower than the Michaelis constant of the interaction. In the present study, therefore, the disposition characteristics of dextran were investigated in detail at three different doses.

Dextran is known to be resistant to metabolic degradation (Mowry & Millican 1953) and ^{14}C-labelled dextran was also shown to be resistant to degradation in the liver of mice (Melton et al 1987). Therefore, the disposition of dextran can be efficiently examined by counting total radioactivity of labelled compound. The present results suggested the existence of a special uptake mechanism for [^{14}C]dextran at a dose of 1 mg kg^{-1}. However, it is not specific for ^{14}C-labelled compound, since liver uptake of [^{14}C]dextran was reduced by co-administration with the native dextran at doses of 10 and 100 mg kg^{-1}.

The glomerular capillary wall functions as a discriminator of molecular size and electric charge (Arturson et al 1971; Taylor & Granger 1984). In the present study, urinary clearance decreased with an increase of the administered dose (Table 1) and the accumulation of dextran in the kidney was negligible at each dose. Dextran consists of a range of mol. wt sugars and the fractions with relatively low mol. wt are rapidly filtered through the glomerulus. Unmodified neutral dextrans with molecular radii less than 20 Å are reported to cross the glomerulus without restriction (Brenner et al 1978). On the other hand, the fractions with higher mol. wt are gradually restricted and dextran with molecular radii larger than 50 Å is scarcely excreted in urine (Leypoldt et al 1987). At a high dose, the liver uptake is saturated and the mol. wt distribution in plasma will be shifted to a high-molecular region with time (Arturson & Wallenius 1964). However, only a small shift would occur at a low dose, since the contribution of urinary excretion is small under these conditions. This can give a rational explanation of the decrease of urinary clearance with an increase of the dose.

Hepatocytes have a receptor for galactose-terminated glycoproteins and efficiently take them up from the circulation (Ashwell & Morell 1974; Ashwell & Harford 1982). On the other hand, Kupffer and endothelial cells are known to have a receptor for mannose-terminated glycoproteins (Smedsrød et al 1990). The galactosylated and mannosylated albumins synthesized by the method of Lee et al (1976) are good candidates for ligands for receptors of the parenchymal and nonparenchymal cells in the liver, respectively (Fujita et al 1990a). In the analysis based on the physiological model, the process of the receptor-mediated hepatic uptake was expressed as a Michaelis–Menten type of saturable process. The hepatic plasma flow, Q, was taken into account since the uptake of Gal-BSA was flow-limited at doses lower than 1 mg kg^{-1} (Nishikawa et al unpublished data). The saturable elimination process from the plasma pool would represent the uptake by organs such as bone marrow and spleen which were reported to take up glycoproteins (Regoeczi et al 1980; Summerfield et al 1982; Jones & Summerfield 1988). In the case of dextran, however, the urinary excretion is the major route of elimination apart from hepatic uptake. The urinary clearance apparently followed non-linear kinetics in the present experiment as mentioned above (Table 1) and this was also included in extrahepatic elimination in the model. In Fig. 5, the apparent hepatic clearance is simulated using equations 2 and 7 with values of $K_{m,l}$, $V_{max,l}$, $K_{m,p}$, and $V_{max,p}$ listed in Table 2 and compared with values in Table 1 which were calculated independently of the model. Good correlation is observed suggesting the present pharmacokinetic model can explain the experimental results (Fig. 3).

In Fig. 4, the plasma concentration and liver accumulation of [^{14}C]dextran (1 mg kg^{-1}) co-administered with Gal-BSA (30 mg kg^{-1}) were stimulated using pharmacokinetic parameters obtained in independent experiments and assuming that Gal-BSA inhibits hepatic uptake but not extra-hepatic elimination of [^{14}C]dextran. The curves obtained are in good agreement with the experimental data (Fig. 5). This result, together with the finding of cellular localization of [^{14}C]dextran in the liver suggests that dextran is taken up by the same

mechanism as Gal-BSA, i.e. via the receptor for asialoglycoprotein. This new finding would explain an increase of the liver uptake of uricase conjugated with dextran observed previously (Fujita et al 1990b).

In the present study, it is suggested that dextran is taken up by the liver via the asialoglycoprotein receptor in mice. The asialoglycoprotein receptor is known to be present in the liver of many mammalian species including man. In man, about 40% of dextran administered as a plasma expander accumulated in the body, probably in the liver (Arturson et al 1964). Hence, the conjugation of drugs with dextran may lead to undesirable accumulation in the liver. In the strategy of optimizing drug delivery by conjugating with macromolecules, however, dextran is still one of the worthwhile carriers (Larsen 1989). Carboxymethylation of dextran is considered a promising approach, since carboxylmethyl-dextran uptake in liver is reduced and plasma concentration is high (Takakura et al 1990). The moderate anionic charge on dextran decreases the interaction with the tissue and prevents the recognition of its sugar residues by the asialoglycoprotein receptor.

References

Arturson, G., Wallenius, G. (1964) The intravascular persistence of dextran of different molecular sizes in normal humans. Scand. J. Clin. Lab. Invest. 1: 76–80

Arturson, G., Granath, K., Thoren, L., Wallenius, G. (1964) The renal excretion of low molecular weight dextran. Acta Chir. Scand. 127: 543–551

Arturson, G., Groth, T., Grotte, G. (1971) Human glomerular membrane porosity and filtration pressure: dextran clearance data analyzed by theoretical models. Clin. Sci. 40: 137–158

Ashwell, G., Harford, J. (1982) Carbohydrate-specific receptors of the liver. Ann. Rev. Biochem. 51: 531–554

Ashwell, G., Morell, A. G. (1974) The role of surface carbohydrates in the hepatic recognition and transport of circulating glycoproteins. Adv. Enzymol. 41: 99–128

Brenner, B. M., Hostetter, T. H., Humes, H. D. (1978) Glomerular permselectivity: barrier function based on discrimination of molecular size and charge. Am. J. Physiol. 234: F455–F460

Fujita, T., Ohtsubo, Y., Nishida, K., Hashida, M., Sezaki, H. (1990a) Pharmacokinetics of receptor-mediated targeting system with sugar moiety. Proc. 17th Int. Symp. Controlled Release Bioact. Mater. 17: 387

Fujita, T., Yasuda, Y., Takakura, Y., Hashida, M., Sezaki, H. (1990b) Alteration of biopharmaceutical properties of drugs by their conjugation with water-soluble macromolecules: uricase-dextran conjugate. J. Contr. Rel. 11: 149–156

Gerlowski, L. E., Jain, R. K. (1983) Physiologically based pharmacokinetic modeling: principles and applications. J. Pharm. Sci. 72: 1103–1127

Hashida, M., Kato, A., Takakura, Y., Sezaki, H. (1984) Disposition and pharmacokinetics of a polymeric prodrug of mitomycin C, mitomycin C-dextran conjugate, in the rat. Drug Metab. Dispos. 12: 482–499

Isbell, H. S., Frush, H. L., Moyer, J. D. (1957) Use of carbon-14 and tritium for the study and characterization of cellulose and other polysaccharide. Tech. Assoc. Pulp. Paper Ind. 40: 739–742

Jones, E. A., Summerfield, J. A. (1988) Kupffer cells. In: Arias, I. M., Jakoby, W. B., Popper, H., Schachter, D., Shafritz, D. A. (eds) The Liver: Biology and Pathobiology. 2nd ed, Raven Press Ltd, New York, pp 683–704

Larsen, C. (1989) Dextran prodrugs—structure and stability in relation to therapeutic activity. Adv. Drug Deliv. Rev. 3: 103–154

Lee, Y. C., Stowell, C. P., Krantz, M. J. (1976) 2-Imino-2-methoxyethyl 1-thioglycosides: new reagents for attaching sugars to proteins. Biochemistry 15: 3956–3963

Leypoldt, J. K., Frigon, R. P., DeVore, K. W., Henderson, L. W. (1987) A rapid renal clearance methodology for dextran. Kidney Int. 31: 855–860

Melton, R. G., Wiblin, C. N., Baskerville, A., Foster, R. L., Sherwood, R. F. (1987) Covalent linkage of carboxypeptidase G2 to soluble dextrans-II: in vivo distribution and fate of conjugates. Biochem. Pharmacol. 36: 113–121

Mowry, R. W., Millican, R. C. (1953) A histological study of the distribution and fate of dextran in tissues of the mouse. Am. J. Pathol. 29: 523–545

Nakane, S., Matsumoto, S., Takakura, Y., Hashida, M., Sezaki, H. (1988) The accumulation mechanism of cationic mitomycin C-dextran conjugates in the liver: in-vivo cellular localization and in-vitro interaction with hepatocytes. J. Pharm. Pharmacol. 40: 1–6

Regoeczi, E., Chindemi, P. A., Hatton, M. W. C., Berry, L. R. (1980) Galactose-specific elimination of human asialotransferrin by the bone marrow in the rabbit. Arch. Biochem. Biophys. 205: 76–84

Sezaki, H., Hashida, M. (1984) Macromolecule-drug conjugates in targeted cancer chemotherapy. CRC Crit. Rev. Ther. Drug Carrier Syst. 1: 1–38

Sezaki, H., Takakura, Y., Hashida, M. (1989) Soluble macromolecular carriers for the delivery of antitumour drugs. Adv. Drug Deliv. Rev. 3: 247–266

Smedsrød, B., Pertoft, H., Gustafson, S., Laurent, T. C. (1990) Scavenger functions of the liver endothelial cell. Biochem. J. 266: 313–327

Summerfield, J. A., Vergalla, J., Jones, E. A. (1982) Modulation of a glycoprotein recognition system on rat hepatic endothelial cells by glucose and diabetes mellitus. J. Clin. Invest. 69: 1337–1347

Takakura, Y., Kitajima, M., Matsumoto, S., Hashida, M., Sezaki, H. (1987a) Development of a novel polymeric prodrug of mitomycin C, mitomycin C-dextran conjugate with anionic charge. II. Disposition and pharmacokinetics following intravenous and intramuscular administration. Int. J. Pharm. 37: 145–154

Takakura, Y., Takagi, A., Hashida, M., Sezaki, H. (1987b) Disposition and tumor localization of mitomycin C-dextran conjugates in mice. Pharm. Res. 4: 293–300

Takakura, Y., Kaneko, Y., Fujita, T., Hashida, M., Sezaki, H. (1989a) Control of pharmaceutical properties of soybean trypsin inhibitor by conjugation with dextran I: synthesis and characterization. J. Pharm. Sci. 78: 117–121

Takakura, Y., Fujita, T., Hashida, M., Sezaki, H. (1989b) Control of pharmaceutical properties of soybean trypsin inhibitor by conjugation with dextran II: biopharmaceutical and pharmacological properties. Ibid. 78: 219–222

Takakura, Y., Fujita, T., Hashida, M., Sezaki, H. (1990) Disposition characteristics of macromolecules in tumor-bearing mice. Pharm. Res. 7: 339–346

Taylor, A. E., Granger, N. D. (1984) Exchange of macromolecules across the microcirculation. In: Renkin, E. M., Michel, C. C. (eds) Handbook of Physiology: The Cardiovascular System IV. American Physiological Society, Bethesda, MD, pp 467–520

Vogel, C. W. (1988) Current approaches of immunotargeting. In: Vogel, C. W. (ed.) Immunoconjugates: Antibody Conjugates in Radioimaging and Therapy of Cancer. Oxford University Press, New York, pp 3–7